ELSEVIER

Food Chemistry 69 (2000) 447–455

Food Chemistry

www.elsevier.com/locate/foodchem

Effects of muscle texture on ultrasonic measurements

Saïd Abouelkaram [a,*], Krzysztof Suchorski [a], Béatrice Buquet [a], Philippe Berge [a], Joseph Culioli [a], Philippe Delachartre [b], Olivier Basset [b]

[a] *Station de Recherches sur la Viande, RST, INRA, Theix, 63122 St. Genès Champanelle, France*
[b] *CREATIS, CNRS Research Unit (UMR 5515), INSA 502, 69621 Villeurbanne Cedex, France*

Received 20 March 1999; received in revised form 31 July 1999; accepted 31 August 1999

Abstract

In this study bovine muscle samples were analysed using an ultrasonic method to investigate the influence of compositional and textural characteristics on ultrasonic measurements. The ultrasonic method was based on the measurement of acoustic parameters (velocity, attenuation and backscattering intensity) which are closely related to physical properties of the propagating medium. An examination of physical parameters was proposed by two types of representations: a mean profile and a parametric image. Two muscle types, which differ in composition and structure were studied. On the same samples additional measurements, mechanical resistance and chemical composition, were performed and used to show the influence of meat composition and texture on ultrasonic data.

1. Introduction

The determination of meat quality is a major problem for the beef industry. As a consequence, there has been a growing interest in the setting up of beef grading methods to assess meat quality objectively. For this purpose ultrasound analysis is recognised as displaying many advantages: it is accurate, rapid, non-destructive, non-invasive, relatively inexpensive, and suitable for on-line industrial applications.

Many studies have already been performed on this subject, and different approaches to beef quality grading are in course. Ultrasound has been used to estimate beef carcass composition (Miles, Fisher, Fursey & Page, 1987; Miles, Fursey, Page & Fisher, 1990) and to study beef sensory attributes (Park, Whittaker, Miller & Hale, 1994). Kim, Amin, Wilson, Rouse, and Udpa (1998) evaluated the marbling pattern or distribution of intramuscular fat (IMFAT) in live beef animals from ultrasound images. The need for an objective evaluation method was reported. Park et al. and Whittaker, Park, Thane, Miller and Savell. (1992) studied the potential use of A-mode and B-mode ultrasound to characterise IMFAT in beef carcasses and Cross and Whittaker (1992) were convinced of the potential of ultrasound to determine beef meat quality.

The composition and structure of the muscle influence meat quality characteristics, such as tenderness, which is of real concern to the beef industry because of its high variability. The industry has a real need for systems able to correctly estimate meat tenderness to both guarantee a constant quality and answer to consumers demand, for whom tenderness is a predominant quality in the choice of purchase.

Tenderness, which has many sources of variability, is highly influenced by connective tissue characteristics. The distribution and the amount of both fat and collagen in the muscle play an important role in the constitution and organisation of the connective tissue, which, according to lipid and collagen contents, displays specific viscoelastic properties. The study of these properties is a way to characterise beef meat quality since collagen contributes to muscle cohesion, and then to its elasticity, and lipids contribute to muscle viscosity.

The propagation of ultrasound in a medium is closely dependent on its mechanical properties. The measurement of some pertinent acoustical parameters allows the mechanical properties of the medium to be characterised. The aim of our study was to investigate the use of ultrasound to characterise the composition and

* Corresponding author. Tel.: +33-4-7362-4551; fax: +33-4-7362-4089.

E-mail address: karam@clermont.inra.fr (S. Abouelkaram).

0308-8146/00/$ - see front matter
PII: S0308-8146(00)00067-4

the structure of bovine muscles. Three ultrasonic parameters (velocity of wave propagation, attenuation and backscattering intensity of the ultrasonic waves) and two types of parameter representations (mean profile and parametric image) were used to analyse global and local characteristics of meat samples.

2. Materials and methods

2.1. Muscles samples

Muscles used were *Triceps brachii* (TB) and *Longissimus dorsi pars thoracis* (LD) of four animals: a 4 year-old Salers culled cow, two 19 month-old bulls from the Salers and Charolais breeds, and a 24 month-old Aubrac bull (Table 1). Muscle sections were frozen 8 days after slaughter and maturation was thus achieved.

2.2. Ultrasonic scanning

Meat samples (10 × 5 × 4.5 cm) were cut from the thawed muscle sections and each mounted inside a plexiglass rectangular box (Fig. 1) with four slits at 2 cm intervals. These slits were made to allow both an easy localisation of the ultrasonic scanning plane and to guide cutting of sample slices to be used for photography. The contained meat samples were embedded in a gelatine gel (15% w/v). Embedding assisted slicing by enhancing sample cohesion. The gel was both transparent for ultrasonic waves and non-scattering.

Table 1
Animals studied[a]

Animal number	Age (months)	Breed
An1	48	Salers
An2	24	Aubrac
An3	19	Charolais
An4	19	Salers

[a] The animals were provided by the CMH Laboratory of INRA (Theix, France).

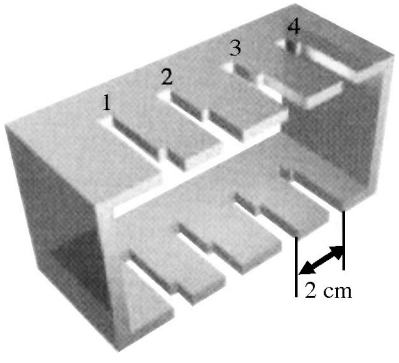

Fig. 1. Plexiglass box.

The ultrasonic bench (Fig. 2) consisted of a prototype echograph "I-scan" and a temperature controlled water tank. The echograph "I-scan" was designed in our laboratory and constructed locally by I+TECH Company (Clermont-Ferrand, France). This echograph was composed of two transducers (5 MHz, 50 mm focal distance) denoted as T1 and T2. Each transducer was sealed in a waterproof box and each attached to its own motor. These motors allowed the displacement of the transducers in one direction to perform the ultrasonic scanning. This linear mechanical scanning reproduced scanning by an array transducer with a low cost equipment.

The two boxes containing the transducers were separated by a distance corresponding to the superposition of the transducers focal planes. The set of these two boxes was able to be moved perpendicularly to the scanning direction by a third motor. This combination of motors allowed the displacement of the transducers in two directions, y and z. The scanning movement of the two transducers was synchronised so that the beams were always aligned.

This configuration allowed recording of the signals, required for computation of ultrasonic parameters, in both transmission and reflection modes. The signal emission was in impulse mode and the received signals were acquired at a sampling frequency of 26 MHz. A third transducer, connected to the echograph, was used to produce signals required to determine the speed of sound in the water bath. The entire bench was controlled by a microcomputer.

Sample scanning was performed at each slit by acquiring A-scans separated by 0.3 mm. Six different signals were recorded: one signal for the determination of speed in water, one for the determination of both echographic images and backscattering intensity (BSI) and the remaining four for the determination of sample speed and attenuation (Atten). The ultrasonic measurements

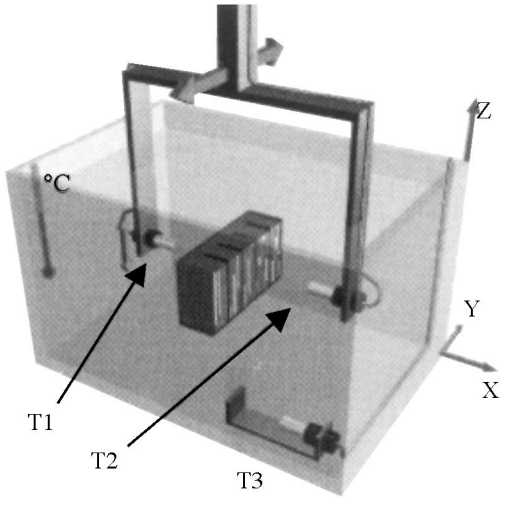

Fig. 2. Ultrasonic bench.

were achieved at 30°C, near the temperature of the animals at slaughter. This temperature was selected to enhance the heterogeneity of the meat, thereby enhancing the intramuscular fat echogenecity.

2.3. Signal analysis

The speed of sound was obtained by first calculating the sample thickness, e. This thickness was divided by the time, ts, required for the wave to traverse the sample and the speed was given by the ratio e/ts.

Wave attenuation α, expressed in dB/cm, was calculated at 1 MHz frequency according to the equation:

$$\alpha = (20^* \log_{10} \frac{S_{\text{sample}}}{S_{\text{water}}})/e$$

where S_{sample} and S_{water} are the calculated spectrum of the signal which has passed through the meat sample and water, respectively. The BSI was obtained by calculating the mean of the squared amplitudes of the same signals used for echographic images.

After acquisition of echographic images, the muscle samples were cut through the slits. Ultraviolet and visible photographic images of the muscle slices were made. This allowed collection of different image types of the same cross-section of the muscle samples.

The imaging system was composed of a CCD camera (SONY MACC-77) mounted on a photographic bench. The camera was connected to a microcomputer equipped with a digitisation card (Matrox Meteor). The images were digitised with a dynamic of 256 gray levels. The images of the slices (4.5 × 5 cm) were digitised (767 × 556 pixels). For each meat slice, two images were acquired, one from each ultraviolet light (365 nm) and the other with visible light at room temperature. The ultraviolet light increased the contrast because of the autofluorescence of the connective tissue.

Mechanical tests were performed on all raw meat slices at 20 and 80% deformation according to Got et al. (1999). The first compression ratio provided information related to myofibre resistance, and the second, to connective tissue resistance.

Total hydroxyproline content (THyd) of the samples was determined by the method described by Bergman and Loxley (1963). Intramuscular neutral lipid content (LIP) was determined by the method described by Arneth (1972). Dry matter (DM) was measured according to the procedure described by Boccard et al. (1981). These chemical measurements were made using the set of sample slices.

2.4. Deconvolution of ultrasonic meat images

Ultrasonic measurements were performed with a single focussed transducer, so that meat images had good resolution in the focussed area. However, these images suffered from a lack of resolution outside this area and deconvolution processing was used to restore the degraded images.

Deconvolution consists of the restoration of the image degraded by the imaging system, in order to approach the real object representation. In other words, image deconvolution consists of resolving the inverse problem of the direct equation expressed as:

$$\begin{aligned} y(i,j) &= \sum_{k=1}^{M}\sum_{l=1}^{N} h(i-k, j-l) f(k,l) + n(i,j) \\ &= h(i,j)^{**} f(i,j) + n(i,j) \end{aligned} \quad (1)$$

where y is the raw image, h is the point spread function of the imaging system, n the noise introduced by the system, the indices i, j, k and l the spatial coordinates of image pixels and the symbol ** denotes the two-dimensional convolution. This equation is valid for space invariant systems but can be applied to space variant systems using a block processing approach.

Among the existing methods (Banham & Katsaggelos, 1997), the direct regularised restoration approach is the most simple way to restore original images. For example, constrained least squares restoration can be formulated by choosing an $\hat{f}$ to minimise the lagrangian:

$$\min\left[\left\|y - H\hat{f}\right\|^2 + \alpha\left\|C\hat{f}\right\|^2\right] \quad (2)$$

where the term $C\hat{f}$ is a high pass filtered version of the image $\hat{f}$. This is essentially a smoothness constraint which suggests that most images have a limited high-frequency activity, and thus it is appropriate to minimise the amount of high-pass energy in the restored image. In Eq. (2), α represents the Lagrange multiplier, commonly referred as the regularisation parameter, which controls the trade-off fidelity to the data expressed as $\left\|y - H\hat{f}\right\|^2$ and the smoothness of the solution expressed as $\left\|C\hat{f}\right\|^2$. The minimisation of Eq. (2) leads to:

$$\hat{f} = \left(H^T H + \alpha C^T C\right)^{-1} H^T y \quad (3)$$

In practice, this equation was solved in the frequency domain:

$$F_i = \frac{H_i^* Y_i}{|H_i|^2 + \alpha |C_i|^2} \quad (4)$$

where H_i, C_i and F_i represent the 2D discrete frequency components of the imaging system, the high pass filter

(constraint operator) and the restored image. A satisfactory estimation of α may be obtained by the cross-validation method (Thompson, Brown, Kay & Titterington, 1991), which consists of minimising the ratio of the bias and the variance of the restored image as a function of the regularisation parameter.

2.5. Tissue characterisation

Standard echographic images were obtained as the envelope image of the ultrasonic signal propagated in a medium. From the radio-frequency (rf) signal, other acoustical features were calculated. These were:

1. the integrated backscatter (IBS) which quantifies the ultrasonic scattering properties of tissues. The IBS is defined as the mean power value over the short local rf signal.
2. the mean central frequency (MCF) of the backscattered echoes from a region of tissue. This feature is a mean estimating the local attenuation coefficient. It is calculated as the centroid of the power spectral density (Baldeweck, Laugier, Herment & Berger, 1995).

These acoustical features depend on the structure of tissues and can constitute a signature of the various tissues. These features were calculated from local radio-frequency signals to build parametric images.

3. Results and discussion

The muscle samples analysed in this study were selected from a set of 40 muscles. This set was composed of different muscles, from bulls and cows of various ages and breeds, selected to obtain a wide range of variation in lipid and collagen contents. The sample subset used was composed of muscles chosen because they exhibit large differences in lipid content and in structure. The sample number was intentionally reduced in order to focus the study on intra-muscular variability.

3.1. Chemical composition

The composition of five muscle samples are presented in Fig. 3. The order of the muscles along the x-axis was selected according to decreasing intramuscular lipid content (Fig. 3a) and was maintained for the analysis of results from mechanical and ultrasonic measurement. It is evident from Fig 3a that animal An1 was fatter than the other three animals studied. In Fig. 3b the dry matter appeared to decrease with decreasing lipid content, except for the LD of animal An4 which showed an unexpectedly high value. However, it was suggested by the ultrasonic measurements that this high value was not an artefact. As expected there were no correlations between hydroxyproline content (Fig. 3c) and either lipid content or dry matter content (Table 2). It was noted that the hydroxyproline content for the LD of animal An2 was high.

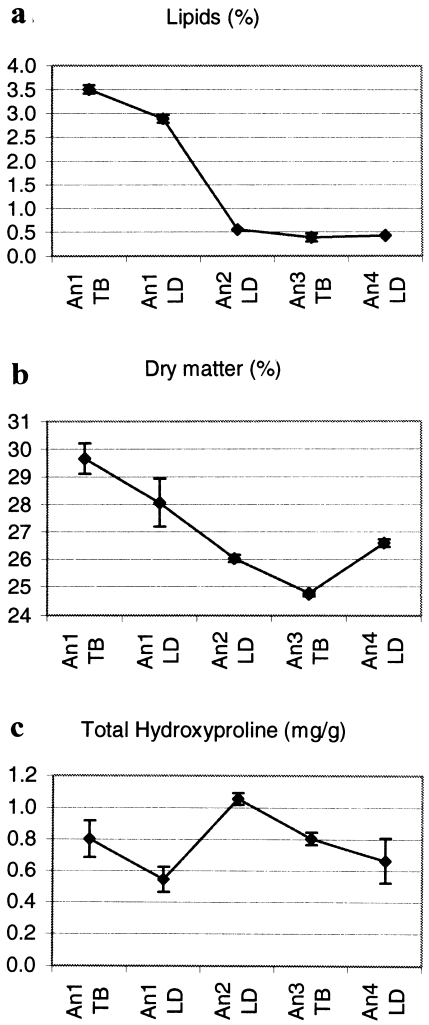

Fig. 3. Chemical compositions of muscle samples: (a) neutral lipids, (b) dry matter and (c) total hydroxyproline.

3.2. Mechanical measurements

The mechanical results of the five samples are presented in Fig. 4. Mechanical resistance measured at 20% of deformation, shown in Fig. 4a, is related to myofibre resistance. No significant differences were observed between the five samples for this parameter which means that the ageing states were similar for the different samples.

The results of compression tests at 80% of deformation are given in Fig. 4b. This measure is related to connective tissue resistance. The TB and LD muscles of animal An1 appeared to be the toughest and softest samples in the set, respectively.

Table 2
Correlation coefficients obtained between ultrasonic, chemical and mechanical parameters

	Atten	BSI	DM	LIP	THyd	K20	K80
Speed	−0.55	−0.75	−0.91	−0.97	0.21	−0.49	−0.42
Atten	1	−0.10	0.84	0.60	−0.21	−0.21	−0.01
BSI		1	0.46	0.71	−0.32	0.85	0.38
DM			1	0.93	−0.32	0.27	0.23
LIP				1	−0.38	0.44	0.19
THyd					1	-0.47	0.52
K20						1	0.41

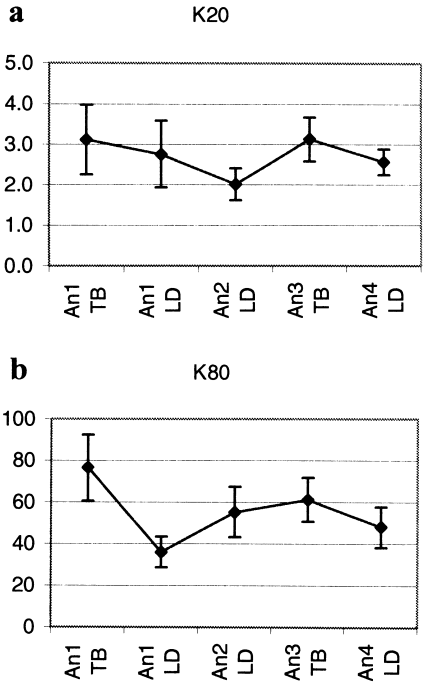

Fig. 4. Mechanical resistance (N/cm^2) at (a) 20% and at (b) 80% of deformation.

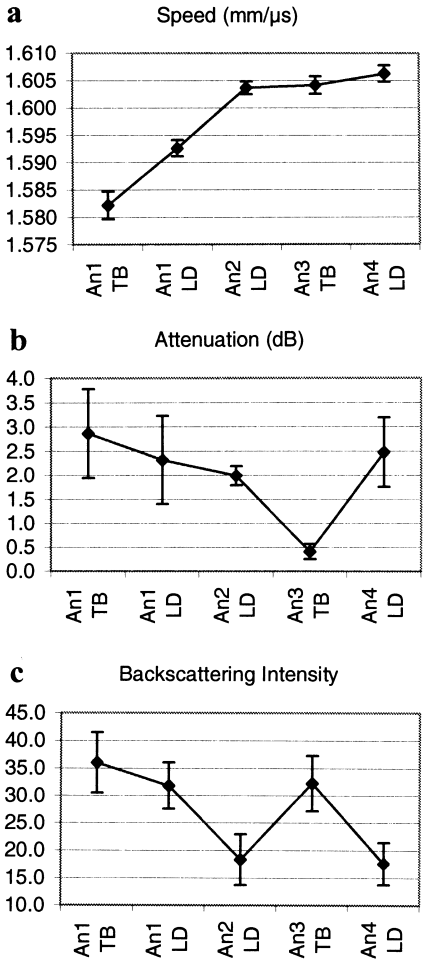

Fig. 5. Total averages of (a) ultrasonic parameters speed of wave, (b) attenuation and (c) backscattering intensity for the five samples.

3.3. Ultrasonic measurements

3.3.1. Global results: composition effect

In this section, the global means of parameters measured in all slits of each sample are presented. These results show the influence of composition on ultrasonic parameters. The ultrasonic results of the five samples are presented in Fig. 5. Muscles from animal An1 exhibit lower speed values than the muscles from the other animals (Fig. 5a). In Fig. 5b the attenuation appeared to decrease with the selected order of the samples, except for the LD of animal An4. No apparent trend was observed in the BSI results (Fig. 5c).

Composition had a direct effect on ultrasonic parameters (Abou El Karam, Berge & Culioli, 1997) which were measured at 30°C. This temperature enhances the lipid effect visible on speed, attenuation and backscattering curves. Indeed, the speed in fat decreases with the temperature (Ghaedian, Coupland, Decker & McClément, 1998; Miles, Fursey & Jones, 1985) and the effect is inverse for a lean tissue. At this temperature a fatty tissue displays lower global speed value than for a leaner tissue. Moreover, this difference in speed propagation makes intramuscular fat more heterogeneous and, therefore, more echogenic, as well as contributing to an increase in the wave scattering effect (Abou El Karam, Buquet, Berge & Culioli, 1997a). The consequences of which are increases in both Atten and BSI parameters with increasing lipid content (note that the lipid content increases in the inverse x-axis order). This is clearly visible in Fig. 5 particularly for the three first samples.

Many factors contribute to the attenuation effect. However, in the case of the muscles from animal An1, the higher attenuation values obtained can be explained by the high fat content causing the tissue to be more viscous and heterogeneous. This contributes to wave absorption and scattering which are the main phenomena acting on wave attenuation in soft tissue.

The correlation coefficients obtained for ultrasonic, chemical and mechanical parameters of the five muscle samples are given in Table 2. It is noteworthy that the correlation coefficients are based on only five samples that were selected for their high degree of variability, which can explain some high values. The highest correlation values were obtained for Speed with both DM and LIP. As expected high correlation coefficients were obtained between LIP and both Speed and BSI parameters. Indeed, at the temperature used in this experiment, fatty samples displayed low speed values and, because of echogenecity, high BSI values. The BSI parameter also appears sensitive to muscle texture since it gave a high correlation coefficient (0.85) with the mechanical parameter, K20.

The low correlation observed between LIP and Atten can be explained by the higher than expected Atten values for both samples An2 LD and An4 LD. These results are not surprising since many factors, not only lipid content, contribute to the attenuation phenomenon. For example, fibre density also contributes to the attenuation effect. This cause of variation is suggested by the correlation (0.84) between Atten and DM.

As shown by the correlation, sample composition has a direct effect on ultrasonic measurements:

- Lipids content influenced mainly Speed and BSI parameters.
- Dry matter content influenced Speed and Atten parameters.
- Total hydroxyproline content appeared to have no significant effect on ultrasonic parameters. This is probably due to its low quantity in muscle compared to dry matter or lipid contents.

3.3.2. Locally averaged results: structure effect

3.3.2.1. Intramuscular fat and structure. The results obtained in each of the four slits and for each sample are presented in this section where the muscle structure effect on ultrasonic data is shown.

Fig. 6 displays the local variations that can be found in each sample demonstrating muscle variability. This variability can be attributed to sample components content and their distribution. The An1 TB and LD samples seem more heterogeneous than An2 LD sample since they displayed larger range variation and dispersion of values. The parameter dispersion reflects the intramuscular variability in muscle structure.

The attenuation parameters appear more sensitive to muscle structure variations. This is clearly visible with the muscles TB and LD of animal An1 and the LD muscle of animal An2. Fig. 7 shows the inherent variability in muscle structure. The high dispersion of attenuation for the TB muscle of animal An1 can be explained by the intrinsic variability of connective tissue and the quantity of intramuscular fat.

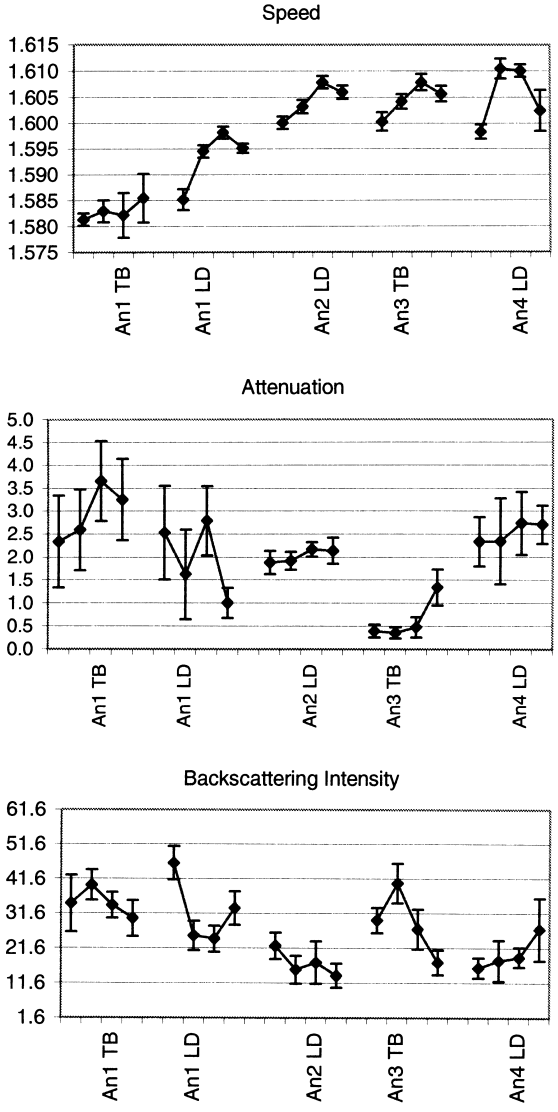

Fig. 6. Averaged ultrasonic parameters obtained in each of the four slits region and for each of the five samples.

In Fig. 7 the images a and b correspond to 2 cm separated slices of the same muscle. These figures illustrate the variations that can be found in muscle structure. The binarised images show both the density of the connective tissue and the importance of intramuscular fat.

As expected, the muscle images of animal An1 revealed a higher elaborated connective tissue, and therefore a higher intramuscular fat deposit, than the image of the LD muscle of animal An2. The lipid contents found by chemical analysis for these muscles were respectively 3.3, 2.9 and 0.4%.

Thus the intramuscular fat has a double effect on ultrasonic measurements:

- its content acts on ultrasonic parameter variation range
- its distribution in connective tissue, acts on ultrasonic parameter dispersion.

These two effects give, respectively, information on constituent content and on muscle structure and therefore on muscle variability.

3.3.2.2. Structure anisotropy. The three samples An2 LD, An3 TB and An4 LD, are the leanest of the set studied and their lipid contents cannot explain the differences observed with ultrasound. As expected, LD and TB muscles exhibited different structures. The results of Atten and BSI, in both Figs. 5 and 6, revealed that the two LD samples had similar values, but these values were completely different from those of TB sample. This difference can be explained by the effect of muscle anisotropy. The consequence of this effect is both higher Atten and speed and lower BSI in the case of propagation of ultrasonic waves along the fibre direction than in the case of a perpendicular propagation to fibre axis direction (Abou El Karam, Buquet, et al., 1997). The images in Fig. 8 show two different fibre alignments which are (a) perpendicular to image plane and (b) parallel to image plane. Note that the ultrasonic waves were propagated in a direction parallel to image plane.

In Fig. 8, two different slices of An3 TB are presented. The differences in their ultrasonic characteristics reflect the different configurations of fibre organisation: (a) in slit 2, the connective tissue stitch which is visible indicates the orthogonal organisation of fibre; (b) in slit 4, fibres are in a layer configuration which is similar to the slice organisation shown in Fig. 9 for LD muscle.

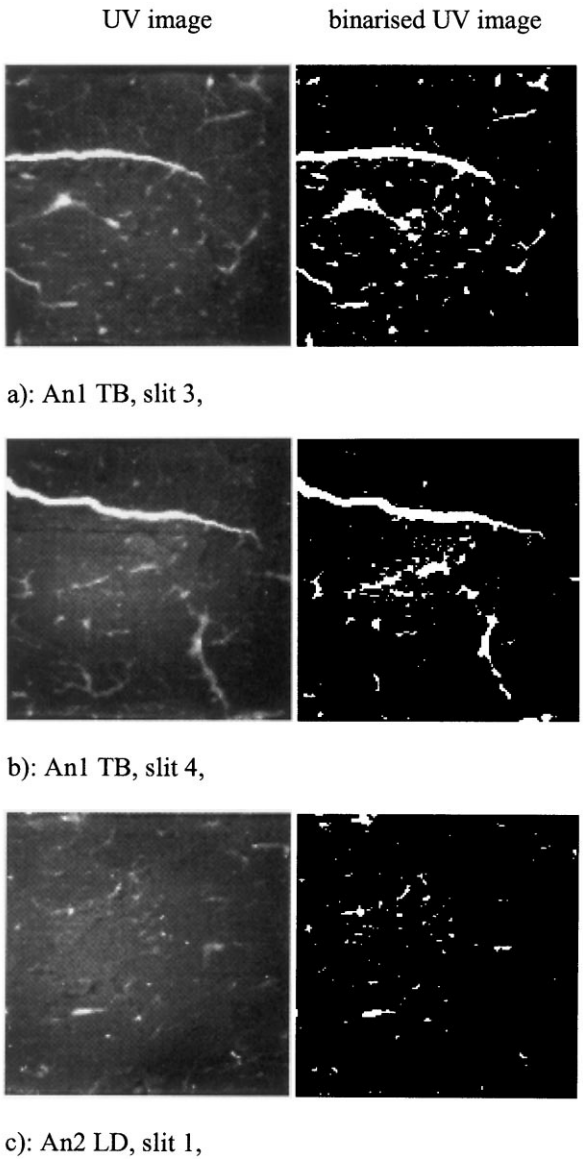

Fig. 7. Images, obtained by UV lighting, of TB and LD muscle slices of animal An1 (slits 3 and 4) and An2 (slit 1).

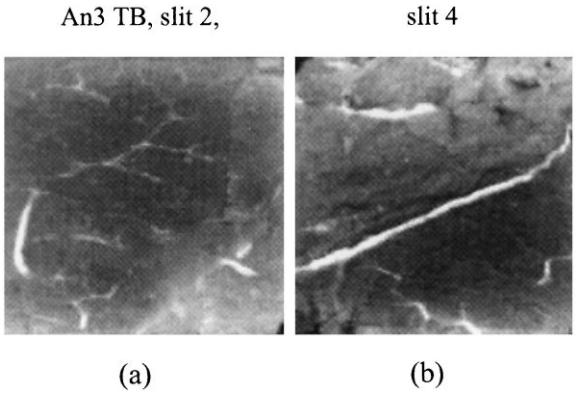

Fig. 8. Images of two slices of animal 3 TB muscle.

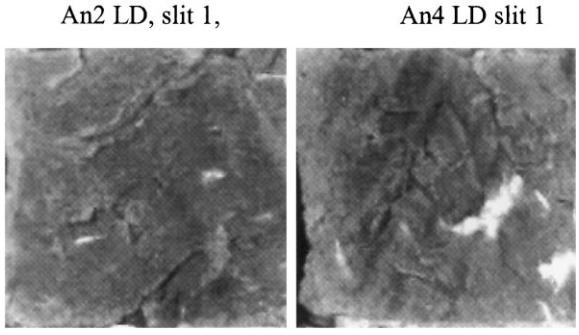

Fig. 9. Images of LD muscle slices of An2 and An4.

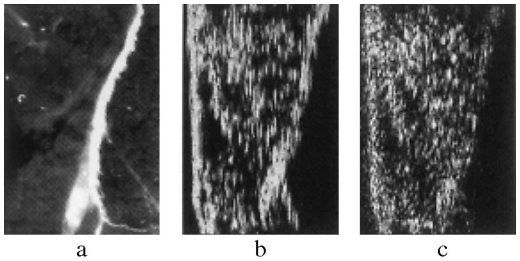

Fig. 10. (a) UV photography and ultrasonic images (b) before (c) and after deconvolution.

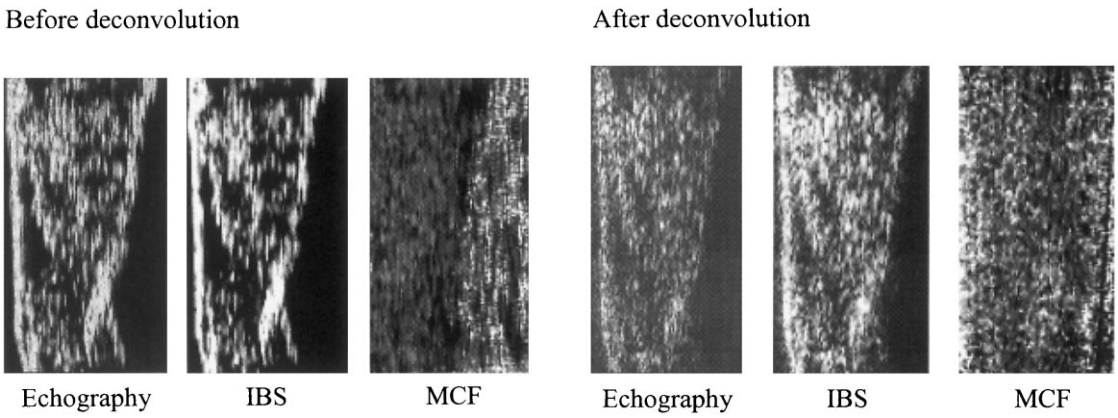

Fig. 11. Comparison of parametric images of a muscle sample, echography, IBS and MCF, before and after deconvolution.

Note that the ultrasonic results, in Fig. 6, of An3 TB in slit 4 are similar to those of An2 LD and An4 LD of which images are shown in Fig. 9.

Fig. 9 clearly shows the fibre layer in the image planes. The highest values of both Atten and BSI are given by this configuration of fibres.

The ultrasonic parameters used are dependent on muscle structure, but are not specific to structure. Because of structure and composition interaction, specific parameters of structure are needed for a better description of muscle tissue. Extraction of parameters from texture analysis of echographic images could help to reach this goal. But the echographic images, acquired with our echograph, contain some problems inherent to this imaging system, which make their exploitation difficult without pre-processing corrections. Among these problems, there are: the loss of resolution outside the focal zone, the tissue structure visibility and the relatively rapid attenuation of signal with wave propagation distance. To solve some of these problems the deconvolution technique was used for image resolution improvement and parametric images, IBS and MCF, were calculated to enhance structure visibility.

3.4. Parametric imaging

In this part, deconvolution pre-processing was made from raw RF images to restore the resolution loss outside the focal area of the focussed transducer. Parameter images based on envelope, IBS and MCF representations were built from a local computation of these parameters on raw RF images and restored images.

The effect of the deconvolution on ultrasonic meat images is illustrated in Fig. 10. The resolution is particularly improved in hyper-echoic area due to strong reflectors (for example, large fatty inclusions). This resolution improvement contributes to a non-fuzzy aspect to the echographic image by introducing high spatial frequencies. It also contributes to an uniform speckle, enhancing the readability comfort of the image. Moreover, the consequence of a regular texture is a decrease in the structure visibility. If the structure detection is less important than restoring resolution, image deconvolution is then recommended.

Another type of improvement of image quality is to enhance structure visibility. For this, the use of IBS or MCF could be useful. Contours of structures are better defined in the IBS image compared to envelope image. Note that slight degradation of axial resolution is observed. On the MCF image, structures are also visible.

The parametric images can also be calculated on the image after deconvolution as illustrated in Fig. 11. Envelope, IBS and MCF parametric images have been calculated before and after deconvolution. As expected deconvolution improves the lateral resolution on IBS images and the echoic structures are better defined. Meat structures are more apparent on both IBS and MCF images before deconvolution. It must be emphasised that, on the right side of the MCF images, the structures appearing are not visible on either envelope or IBS images, because of attenuation of signal. This property of MCF could be useful for restoring information drowned in noise by signal attenuation. Thus, IBS and MCF images can be used as complementary parametric images to reveal meat structures.

4. Conclusions

The influences of sample composition and muscle structure on ultrasonic parameters were shown. The variability in muscle structure, clearly visible in photographic images, was shown by analysis of dispersion of ultrasonic data. Relatively high correlation coefficients were obtained in spite of the high variability existing in the muscle structure.

The ultrasonic method used which is robust enough has a real potential for muscle tissue characterisation and is a promising tool for meat characterisation because of the ability to enhance characteristics, such as

heterogeneity, by changing physical measurement conditions. However, before it can be concluded that this technique has potential in predicting some meat quality traits, further development of the technique and confirmation of the results of the present study on a larger number of samples is necessary.

Moreover, because of the complex nature of muscle tissue, it is necessary to combine several ultrasonic parameters to extract the sample characteristics of composition and structure. Furthermore, with the only ultrasonic parameters used the problem of interaction between composition and structure is not completely solved. This problem will require the use of additional parameters specifically related to structure such as features issued from texture analysis of echographic images.

Acknowledgements

Special thanks to Dr. Tania Ngapo for her precious help. The authors also thank Lenaïck Jehannin for her helpful assistance, R. Fournier and B. Dominguez for the chemical and mechanical analysis. This work has been supported by the European Union (AIR project CT96-1107).

References

Abou El Karam, S., Berge, P., & J. Culioli, J. (1997) Application of ultrasonic data to classify bovine muscles. In: *Proceedings of IEEE ultrasonics symposium* (Vol. 2) (pp. 1197–1200).

Abou El Karam, S., Buquet, B., Berge, P., & Culioli, J. (1997). Ultrasonic characterization of bovine muscles. In: *Proceedings of the* 43rd (ICOMST) (pp. 310–311).

Arneth, W. (1972). Uber die refraktometrische schnellfettbestimmung nach rudisher in fleisch und fleischwaren. *Fleischwirtsch, 52*, 1455–1458.

Baldeweck, T., Laugier, P., Herment, A., & Berger, G. (1995). Application of autoregressive spectral analysis for ultrasound attenuation estimation. *IEEE Trans. Ultrason. Ferroelec. Freq. Cont., 42*(1), 99–109.

Banham, M. R., & Katsaggelos, A. K. (1997). Digital image restoration. *IEEE Signal Processing Magazine, 14*(2), 24–41.

Bergman, I., & Loxley, R. (1963). Two improved and simplified methods for the spectrophotometric determination of hydroxyproline. *Analytical Chemistry, 35*, 1961–1965.

Boccard, R., Butcher, L., Casteels, E., Cosentino, E., Dransfield, E., Hood, D. E., Joseph, R. L., McDougall, D. B., Rhodes, D. N., Schön, I., Tinbergen, B. J., & Touraille, C. (1981). Procedures for measuring meat quality characteristics in beef production experiments. *Livestock Products Science, 8*, 385–397.

Cross, H. R., & Whittaker, A. D. (1992). The role of instrument grading in a beef value-based marketing system. *Journal of Animal Science, 70*, 984–989.

Ghaedian, R., Coupland, J. N., Decker, E. A., & McClément, D. J. (1998). Ultrasonic Determination of fish composition. *Journal of Food Engineering, 35*, 323–337.

Got, F., Culioli, J., Berge, P., Vignon, X., Astruc, T., Quideau, J. M., & Lethiecq, M. (1999). Effects of high intensity high frequency ultrasound on ageing rate, ultrastructure and some physico-chemical properties of beef. *Meat Science, 51*, 35–42.

Kim, N., Amin, V., Wilson, D., Rouse, G., & Udpa, S. (1998). Ultrasound image texture analysis for characterizing intramuscular fat content of live beef catle. *Ultrasonic imaging, 20*, 191–205.

Miles, C. A., Fisher, A. V., Fursey, G. A. J., & Page, S. J. (1987). Estimating beef carcass composition using the speed of ultrasound. *Meat Science, 21*, 175–188.

Miles, C. A., Fursey, G. A. J., & Jones, R. C. D. (1985). Ultrasonic estimation of solid/liquid ratios in fats, oils and adipose tissue. *Journal of the Science of Food and Agriculture, 36*, 215–228.

Miles, C. A., Fursey, G. A. J., Page, S. J., & Fisher, A. V. (1990). Progress towards using the speed of ultrasound for beef leanness classification. *Meat Science, 28*, 119–130.

Park, B., Whittaker, A. D., Miller, R. K., & Hale, D. S. (1994). Ultrasonic spectral analysis for beef sensory attributes. *Journal of Food Science, 59*, 697–701,724.

Thompson, A. M., Brown, J. C., Kay, J. W., & Titterington, D. M. (1991). A study of methods of choosing the smoothing parameter in image restoration by regularization. *IEEE Transactions on Pattern Analysis and Machine Intelligence, 13*(4), 326–339.

Whittaker, A. D., Park, B., Thane, B. R., Miller, R. K., & Savell, J. W. (1992). Principles of ultrasound and measurement of intramuscular fat. *Journal of Animal Science, 70*, 942–952.